

### **Chapter 3**

#### ***Turn-to-Turn Dimerizations of Hairpin Polyamides on Duplex DNA Templates and on NCP Templates***

**Abstract**

Double-helical DNA accelerates the rate of ligation of two six-ring hairpin polyamides, which bind adjacent sites in the minor groove via Michael additions and 1,3-dipolar cycloadditions to form turn-to-turn dimers. The rate of the templated reaction is dependent on DNA sequence as well as on the distance between the hairpin binding sites. Turn-to-turn ligation is also being explored across the “supergroove” of a nucleosome core particle (NCP). Progress towards a fluorescent readout of templated dimerization is also reported.

## Introduction.

Hairpin polyamides have proven useful in binding predetermined sequences of DNA in a sequence-specific fashion.<sup>1-3</sup> Furthermore, this class of molecules has been shown to inhibit the binding of many DNA-binding proteins *in vitro*.<sup>4-11</sup> For the *in vivo* use of these molecules to be realized, they must be able to transverse the cellular and nuclear membranes of live cells in order to reach their target DNA.<sup>12, 13</sup>

For applications in gene regulation within biological systems, binding-site size may be critical because longer sequences should occur less frequently in a gigabase-sized genome. For this reason, the design of ligands capable of targeting >10 base pairs of DNA remains an important goal in the area of polyamide design.<sup>3, 14-16</sup> One approach to increase polyamide binding-site size has been to covalently link two hairpin modules to form hairpin dimers. Dimers linked both “turn-to-tail” and “turn-to-turn” have excellent affinity and specificity to DNA sequences up to 10 bp in length.<sup>17-19</sup> Though likely satisfying the DNA-binding criteria to target unique sequences within genomic DNA, hairpin dimers do not possess the favorable cell and nuclear uptake properties of smaller hairpins, presumably due to size and shape.<sup>12, 13</sup>

In the preceding chapter of this thesis, we demonstrated that duplex DNA can template the formation of “turn-to-tail” tandem hairpin dimers from azide- and alkyne-functionalized hairpin precursors via a 1,3-dipolar cycloaddition reaction.<sup>20</sup> These data showed that tandem-type polyamides capable of targeting sequences of DNA >10 bp could be created from small hairpin starting materials that possess more favorable nuclear localization properties than their dimer products, which will be necessary for *in vivo*

applications. It was found, however, that while alkyne-functionalized polyamides were able to localize to live cell nuclei, polyamides functionalized with azide moieties on the C-terminus were excluded from the nuclei in most cell lines tested. While the azide moiety itself appears to be a negative determinant of nuclear localization, it was found that when the azide is switched from the C-terminus to the internal  $\gamma$ -aminobutyric acid “turn” position, a significant increase in nuclear localization was observed.

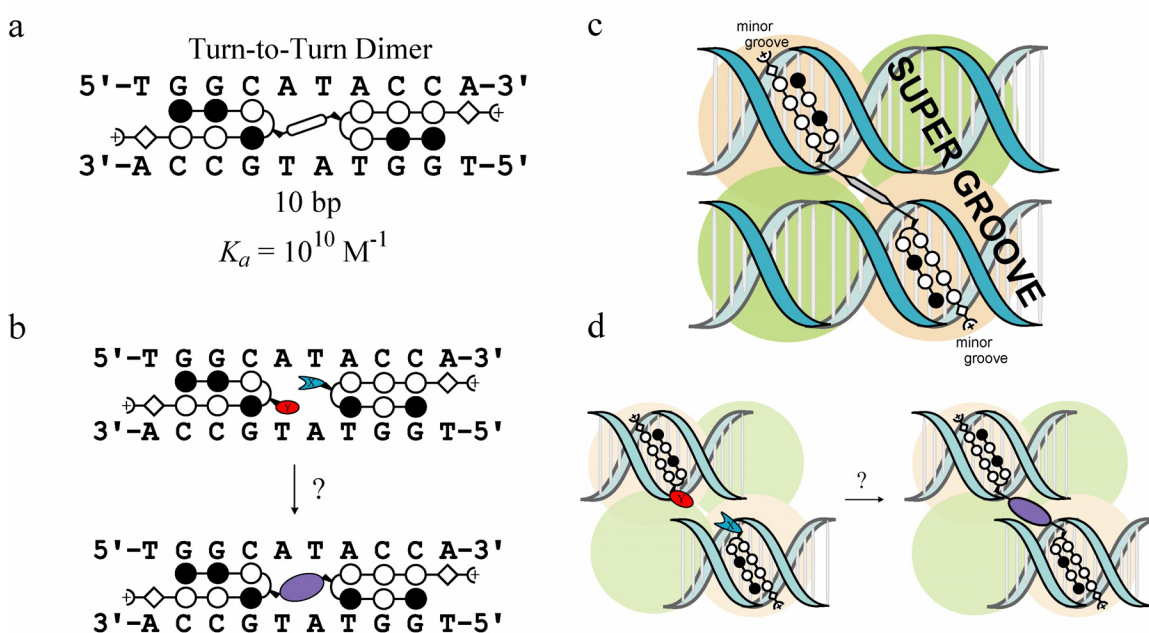


**Figure 3.1.** **a.** Schematic representation of a turn-to-turn hairpin dimer found to bind the 10 base pair sequence shown with  $10^{10}$  binding affinity. **b.** Schematic representation of DNA-templated turn-to-turn dimerization; polyamides functionalized with complementary reactive groups “x” (blue shape) and “y” (red shape) bind DNA. The close proximity of x and y causes a covalent linkage to form between the two polyamides (purple shape). **c.** Schematic representation of “supergroove” recognition by turn-to-turn polyamide dimers. **d.** Schematic representation of how DNA bound to the NCP might template the dimerization of hairpin polyamides bound to a “supergroove.” Here, polyamide binding sites located 80 linear base pairs apart are placed in close proximity upon winding around the nucleosome core proteins. In each figure, pyrrole is represented by open circles, imidazole by closed circles.

Turn-to-turn hairpin dimers have been shown to bind the minor groove of B-form DNA<sup>19</sup> as well as the “supergroove” created when DNA is packaged into nucleosome core particles (Figure 3.1).<sup>21</sup> Because of these successes, coupled with our cell uptake

data, we ask whether DNA is able to template the dimerization of hairpin polyamides in a “turn-to-turn” fashion. In the turn-to-turn orientation, hairpin polyamide starting materials will be functionalized only at the turn position, which, in our previous work was shown to be optimal for nuclear localization. Perhaps this architecture will produce molecules capable of entering the nuclei of live cells, and using the genomic DNA to template the formation of “turn-to-turn” hairpin dimers that target large, genomically unique sequences of DNA (Figure 3.1).

### **Experimental Design.**

Because our previous work indicated that the azide moiety is a negative determinant of nuclear uptake,<sup>22</sup> the scientific literature was searched in order to find other water-compatible organic reactions that do not require additional cofactors or catalysts.<sup>23, 24</sup> The 1,3-dipolar cycloaddition between an azide and an alkyne is not the only reaction that fits the above criteria. One can envision templated dimerizations through a wide variety of reactions such as the Diels-Alder reaction, Michael addition, S<sub>N</sub>2 nucleophilic substitution, or Wittig reaction. Any of these reactions may produce templated dimers from functionalized hairpin polyamides capable of entering live cell nuclei (Figure 3.2).

Because turn-to-turn dimers have been shown to bind two distinct DNA architectures, we are interested in whether the two architectures will have different templating properties. The minor groove of B-form DNA is narrow, and will not accommodate steric bulk.<sup>25-27</sup> Furthermore, each single base pair rise offers approximately 5 Å across which the “turn-to-turn” templated reaction may occur.

Conversely, the gap between the two gyres of DNA on the nucleosome core particle is deep and wide, and may be able to accommodate bulky groups.<sup>28</sup> Structural data shows that the gap between two 8-ring polyamides bound to a nucleosomal “supergroove” is 11 Å. Because of their different molecular structures, these two DNA architectures should have different templating properties. We begin our studies examining the templating properties of linear, duplex DNA.

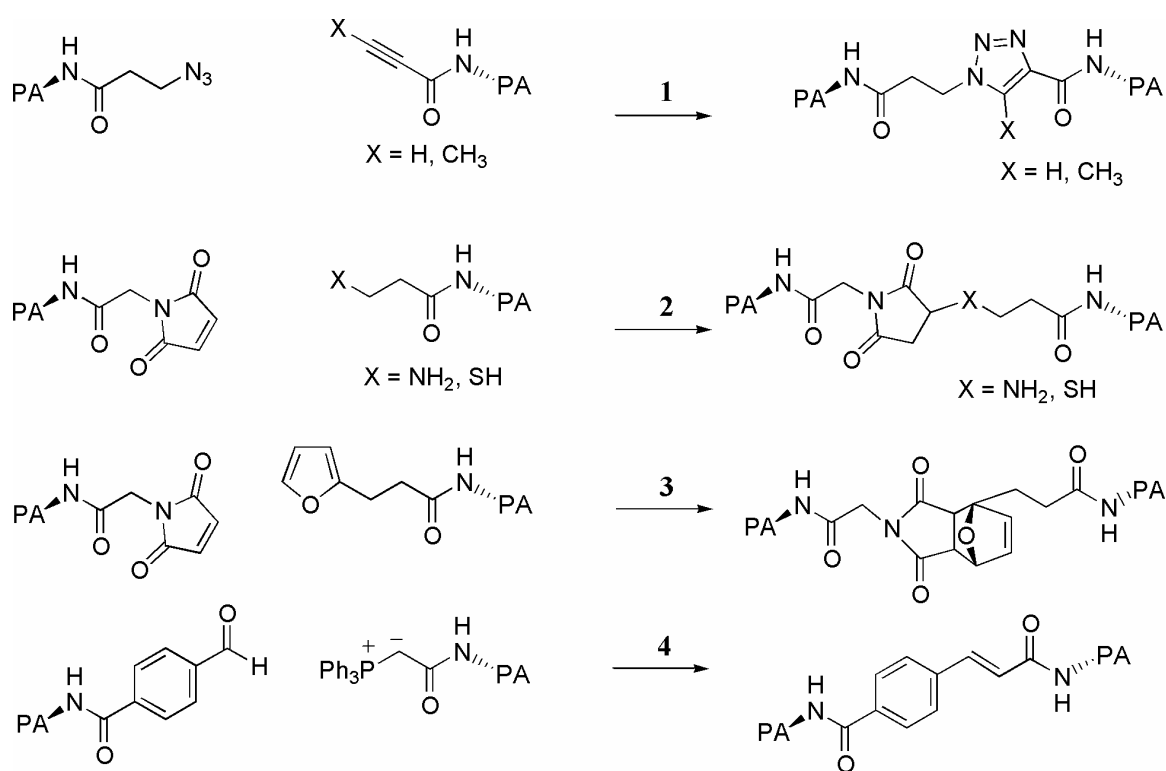


**Figure 3.2.** Structures of several dimerization reactive partners and the putative linkers that form upon dimerization. **1.** 1,3-dipolar cycloaddition forms a triazole linker. **2.** Michael addition forms a cycle-containing linker. **3.** Diels-Alder reaction forms a linker containing a bulky fused ring system. **4.** Wittig reaction forms an unsaturated C-C bond-containing linker.

### Polyamide Design and Synthesis.

Figure 3.3 shows the chemical structures of the functionalized hairpin polyamides synthesized for this study. Unfunctionalized polyamides **1** and **2** were

synthesized on solid support<sup>29, 30</sup> and liberated from resin using dimethylamino propylamine (Dp), leaving a single free amine on the turn residue. Polyamides were then functionalized either with N-hydroxysuccinimidyl esters of the functional groups, or by *in situ* activation of carboxylic acids with PyBOP.

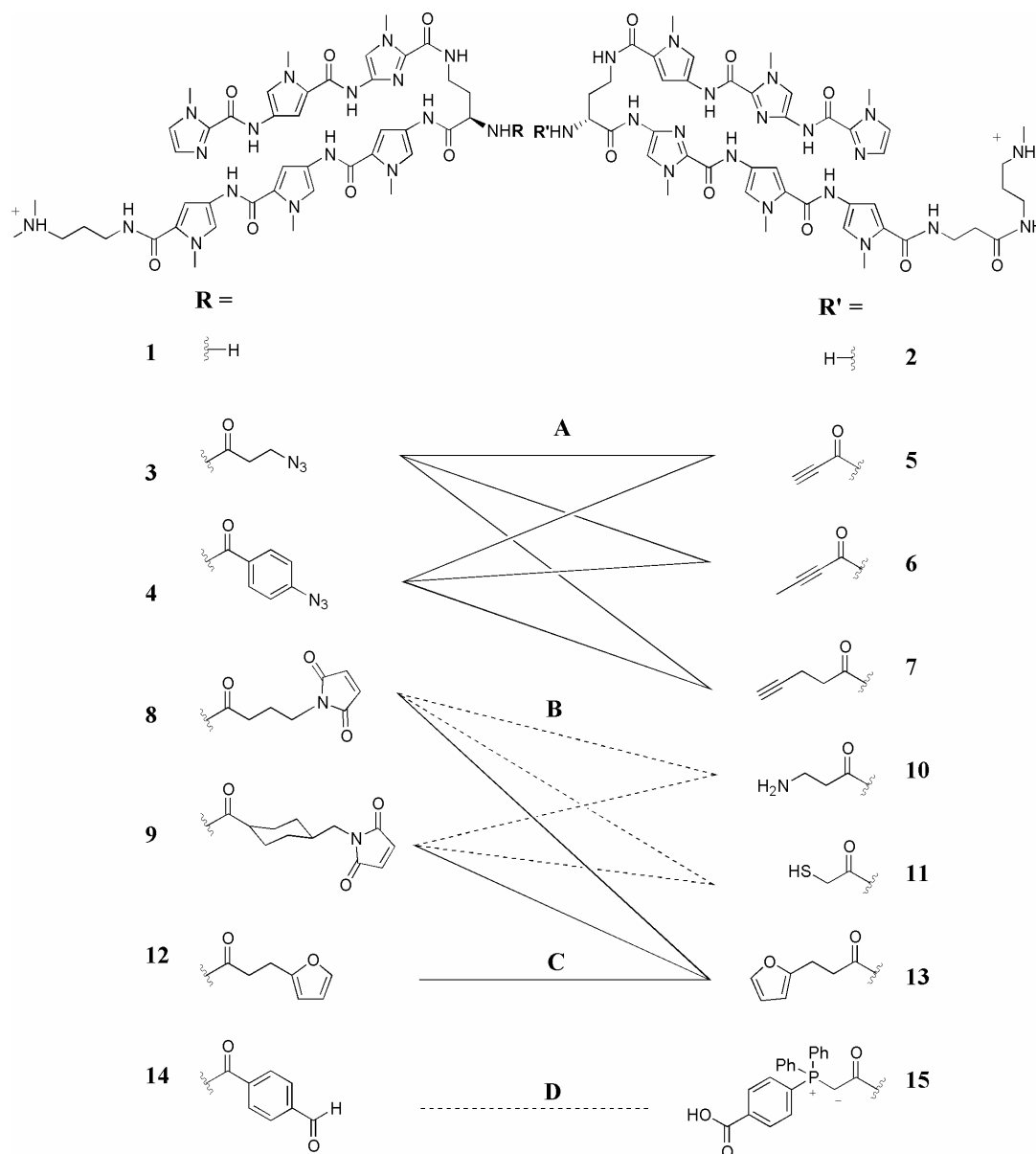


**Figure 3.3.** Chemical structures of the polyamides synthesized for turn-to-turn dimerizations on duplex DNA. Compounds 1 and 2 were synthesized on solid support. Molecules 3–15 were synthesized by amide bond-formation between the turn amines on 1 and 2 and activated esters containing each of the side chains. Lines between columns indicate potential reactive partners via dipolar cycloadditions (A), Michael additions (B), Diels-Alder reactions (C), or the Wittig reaction (D).

Several polyamides were created with identical reactive groups, but with side chains of varying length and steric bulk. These differences were designed into the ligands in order to exploit the molecular differences between linear and nucleosomal DNA templates, thereby leading to molecules that may be capable of specifically forming dimer product on only one of the two architectures (e.g., polyamides **5** and **6** each contain the maleimide reactive group. However, **5** contains a small alkyl linker while **6** incorporates a bulky cyclohexyl linker. Perhaps **5** will react well within the confines of the narrow minor groove while **6** will be sterically excluded from linear DNA, reacting only across the spacious “supergroove”).

#### DNA-Templated Dimerization on Linear, Duplex DNA.

Initial studies were designed to test the ability of match and mismatch linear DNA to template the various turn-to-turn dimerizations. It is anticipated that the spacing



**Figure 3.4.** Sequences of the duplex oligonucleotides containing the match sites for each of the two hairpin polyamides separated by zero, one, two, or three base pairs (A–D, respectively). Duplex E contains a formal polyamide mismatch under each of the two hairpin binding sites (which are separated by zero base pairs). Sequences are listed with the top strand oriented in the 5'→3' direction. Hairpin binding sites are boxed in gray. Mismatch bases are highlighted in red.

between the hairpin binding sites will influence the rates of the templated reactions. To assess the optimal polyamide separation distance, the duplex templates 5'-GGGGTAGGCATCACATGGGG-3' (**A**), 5'-GGGGTAGGCATTCACATGGGG-3' (**B**), 5'-GGGGTAGGCATTTACATGGGG-3' (**C**), 5'-GGGGTAGGCATATTCA-CATGGGG-3' (**D**), were synthesized (Figure 3.4). Each template contains five base pair match sites for each of the hairpin polyamides **1** and **2**, separated by zero, one, two, or three base pairs, respectively.

Initially, each reaction was screened for high templated:nontemplated yield ratios. Reactions were performed with equal concentrations of each hairpin polyamide and DNA (2 mM Tris-HCl, 2 mM KCl, 2 mM MgCl<sub>2</sub>, 1 mM CaCl<sub>2</sub>, pH 7.0, 37 °C. If a nucleophilic amine was involved, reactions were performed in 2 mM Tris-HCl, 2 mM KCl, 2 mM MgCl<sub>2</sub>, 1 mM CaCl<sub>2</sub>, pH 8.2, 37 °C. If a nucleophilic sulfur was involved, reactions were performed in 2 mM Tris-HCl, 2 mM KCl, 2 mM MgCl<sub>2</sub>, 1 mM CaCl<sub>2</sub>, pH 7.4, 37 °C). Reactions were monitored by analytical reversed-phase HPLC. MALDI-TOF MS was used to verify product formation.

Data for the initial templated reaction screen are summarized in Table 3.1. Neither the Wittig (polyamides **14** + **15**) nor the Diels-Alder (polyamides **8** + **13**, **9** + **13**, and **12** + **13**) reactions form detectable amounts of product on any of the four match templates at 1 μM concentrations in a 24-hour period. The Michael additions with the sterically small maleimide **8** (polyamides **8** + **10**, and **8** + **11**) exhibit product formation on both the 10- and 11-base pair templates (**A** and **B**) at 1 μM concentrations, with the reactions proceeding to 7% and 13% (**8** + **10**), and 23% and 26% (**8** + **11**), respectively, in 24 hours. However, under non-templated conditions, products also form in

approximately 5% (**8 + 10**) and 15% (**8 + 11**) yields in 24 hours. Michael additions with the bulky maleimide **9** (polyamides **9 + 10**, and **9 + 11**) were also observed in the absence of template, achieving 5% (**9 + 10**) and 15% (**9 + 11**) yields in 24 hours. However, all four DNA templates produced no reaction between these polyamides in 24 hours.

**Table 3.1.** Tandem product formation after 24 hours.<sup>[a, b]</sup>

	5'- <u>AGGCATCACT</u> -3'	5'- <u>AGGCATTCACT</u> -3'	5'- <u>AGGCATTTCACT</u> -3'	5'- <u>AGGCATATTCACT</u> -3'	No DNA
	<b>A</b>	<b>B</b>	<b>C</b>	<b>D</b>	
<b>3 + 5</b>	<b>78%</b>	<b>37%</b>	---	---	---
<b>3 + 6</b>	<b>35%</b>	---	---	---	---
<b>3 + 7</b>	<b>5%</b>	<b>4%</b>	---	---	---
<b>4 + 5</b>	---	---	---	---	---
<b>4 + 6</b>	---	---	---	---	---
<b>4 + 7</b>	---	---	---	---	---
<b>8 + 10</b>	<b>7%</b>	<b>13%</b>	---	---	<b>5%</b>
<b>8 + 11</b>	<b>23%</b>	<b>26%</b>	---	---	<b>15%</b>
<b>9 + 10</b>	---	---	---	---	<b>5%</b>
<b>9 + 11</b>	---	---	---	---	<b>15%</b>
<b>8 + 13</b>	---	---	---	---	---
<b>9 + 13</b>	---	---	---	---	---
<b>12 + 13</b>	---	---	---	---	---
<b>14 + 15</b>	---	---	---	---	---

<sup>[a]</sup> The assays were carried out at 37 °C at pH 7.0 in the presence of 3 mM Tris-HCl, 3 mM KCl, 3 mM MgCl<sub>2</sub>, and 1.7 mM CaCl<sub>2</sub>, 1 μM each polyamide, 1 μM DNA. <sup>[b]</sup> Yield was quantitated from analytical HPLC traces taken at 24 hours after reaction initiation. Dashed lines indicate no product detected.

1,3 dipolar cycloadditions with the sterically bulky azide **4** (polyamides **4 + 5**, **4 + 6**, and **4 + 7**) produce no dimer product in the absence of template, nor with any of the four duplex templates.

The 1,3 dipolar cycloadditions with the sterically small azide **3** (polyamides **3 + 5**, **3 + 6**, and **3 + 7**) produce no dimer product under non-templated conditions at 1  $\mu\text{M}$  concentrations. When **3** and **7** are incubated with template **A** or **B** at 1  $\mu\text{M}$  concentrations, product is detected after 24 hours (37 °C). Quantitation of HPLC data indicates that the reaction proceeds in approximately 5% yield in 24 hours on each template. No reaction is observed on templates **C** or **D**.

When polyamides **3** and **5** are incubated with templates **A** or **B** at 1  $\mu\text{M}$  concentrations, product is detected after 45 minutes (37 °C). Quantitation of HPLC traces indicate that, after 24 hours, template **A** yields 78% product while template **B** yields 37% dimer product. No reaction is observed on templates **C** and **D**.

When polyamides **3** and **6** are incubated with template **A** at 1  $\mu\text{M}$  concentrations, dimer product is observed in 35% yield after 24 hours. No reaction is observed on templates **B**, **C**, or **D**.

### Reaction Order (Table 3.2).

**Table 3.2.** Pseudozero-order rate constants for the 1,3-dipolar cycloaddition between polyamides **3** and **5**.<sup>[a,b]</sup>

<b>3 + 5</b>	5'- <u>AGGCATCACT</u> -3' <b>A</b>	5'- <u>AGGCATTCACT</u> -3' <b>B</b>	5'- <u>AGGGATGACT</u> -3' <b>E</b>	No DNA
<b>1 <math>\mu\text{M}</math></b>	25,400	9360	8270	$\leq 1$
<b>500 nM</b>	25,300	11700	2520	$\leq 1$

<sup>[a]</sup> The assays were carried out at 37 °C at pH 7.0 in the presence of 3 mM Tris-HCl, 3 mM KCl, 3 mM MgCl<sub>2</sub>, and 1.7 mM CaCl<sub>2</sub>, 1  $\mu\text{M}$  each polyamide, 1  $\mu\text{M}$  DNA. <sup>[b]</sup> Rate constants were calculated from the slope of the first four data points (4.5 hours) when % completion is plotted as a function of time.

Because the 1,3-dipolar cycloaddition between **3** and **5** possesses the most favorable templated yields (while producing no dimer product under nontemplated

conditions), the kinetics of this reaction were studied in depth. Using analytical HPLC, reactions were quenched and quantitated every 1.5 hours for 12 hours. Reaction on template **A** produces 16% dimer product in 1.5 hours, while reaction on template **B** produces 9% product in the same time (Figure 3.5).

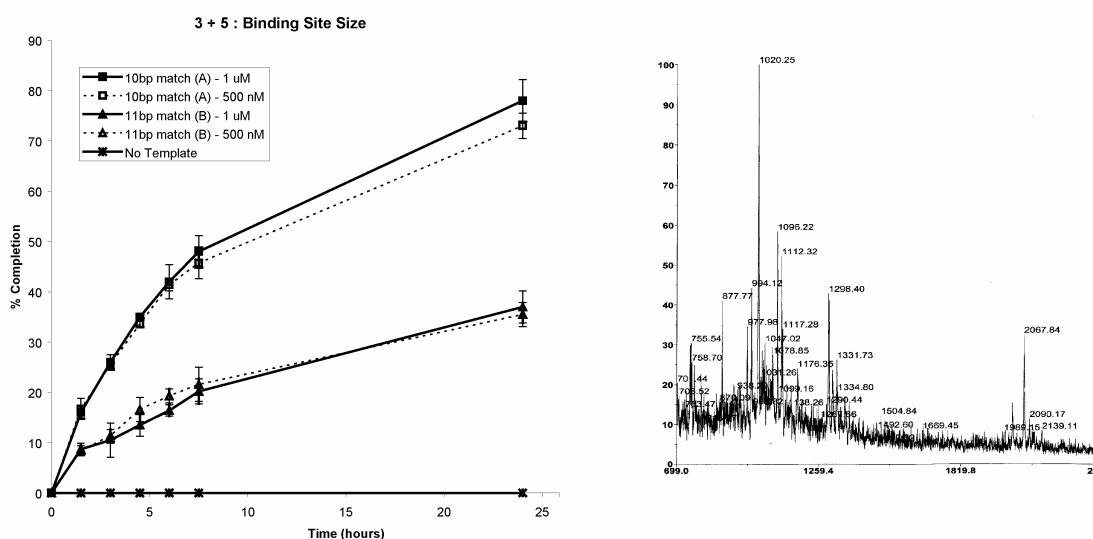


**Figure 3.5.** Left panel: Rate data for the 1,3-dipolar cycloaddition between azide-functionalized polyamide **3** and alkynyl amidate-functionalized polyamide **5** at 1  $\mu$ M and 500 nM concentrations on templates **A** and **B**. Rates of product formation at the two different concentrations are identical, indicating pseudo zero-order kinetics. Right panel: MALDI-TOF mass spectrometry data taken from the reaction of **3** and **5** on duplex template **A** after 8 hours. Product mass is expected at 2067.3  $[M + H]^+$ .

Similarly, when **3** and **5** are incubated with turn-to-turn templates **A** and **B** at 500 nM concentrations, the rates and yields of reactions on these match templates are identical to those at 1  $\mu$ M. Thus, the reaction is independent of concentration, and thus, is a unimolecular process. By plotting product formation as a function of time, pseudozero-order rate constants can be obtained for these reactions. Template **A** increases the rate of dimer formation relative to the non-templated reaction approximately 25,000-fold. Likewise, template **B** increases the rate of dimer formation approximately 10,000-fold.

### Template Mismatch Tolerance: 10 Base Pair Binding Site.

To assess if the cycloaddition reaction between **3** and **5** is sequence-specific with respect to the template, the duplex corresponding to 5'-GGGGTAGGGATGACATG-GGG-3 (**E**) was synthesized. This duplex contains the 10 base pair binding site (zero intervening bases) with a single mismatch (*italicized*) under each of the five base pair hairpin polyamide binding sites. The 10 base pair site was chosen for these studies because site-separation preference results indicate this site to be optimal for product formation.

When **3** and **5** are incubated with mismatch oligo **E** at 1  $\mu\text{M}$  concentrations, product is formed approximately 4-fold slower than on template **A**, eventually achieving 25% yield after 24 hours. When **3** and **5** are incubated with **E** at 500 nM concentrations, the rate is reduced by an additional 4-fold versus the reaction on match template **A**, thereby achieving more than 10-fold match versus mismatch selectivity (Figure 3.6).

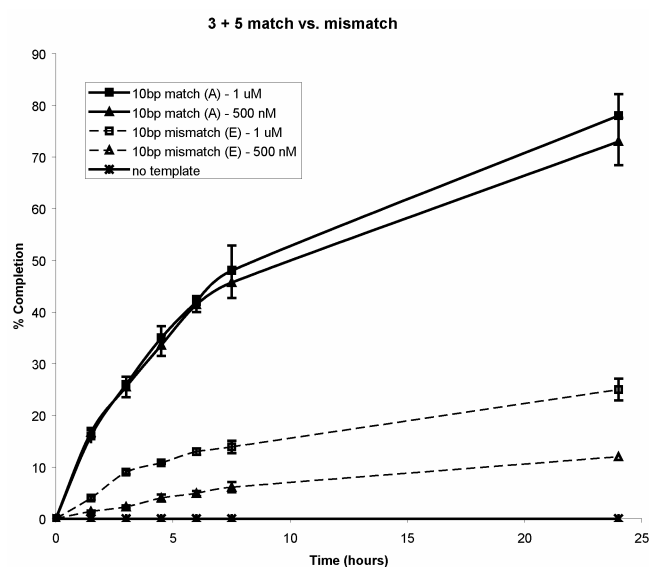


**Figure 3.6.** Rate data for the 1,3-dipolar cycloaddition between polyamides **3** and **5** on the 10 base pair match template (**A**) and the 10 base pair mismatch template (**E**) at 1  $\mu\text{M}$  and 500 nM concentrations. At 500 nM, the reaction proceeds 10 times faster on the match template than on the mismatch template.

### **Towards “Supergroove”-Templated Turn-to-Turn Dimerizations.**

Research has shown that the 146 and 147 base pair duplex DNAs derived from human  $\alpha$ -satellite DNA forms well-positioned nucleosome core particles (NCP) with the histone proteins.<sup>21, 28, 31</sup> Furthermore, cocrystal structures were obtained of these NCPs and various polyamides. Strikingly, because of the palindromic nature of the DNA, a single polyamide was shown to bind two sites located 80 linear base pairs apart, yet juxtaposed in a single “supergroove” by the two gyres of DNA wound around the histone protein core.<sup>28</sup> Subsequent studies linked these two polyamides in a turn-to-turn fashion, forming a homodimeric nucleosome clamp.<sup>21</sup> This clamp was able to effectively prevent NCP melting by locking a full circle of DNA onto the NCP. These types of NCP clamps could have interesting uses for gene silencing in living systems. However, the clamps are branched oligomers of large size and, as such, are unable to translocate across cellular and nuclear membranes.<sup>12</sup> Perhaps the NCP can be used to template the formation of clamplike turn-to-turn dimers from cell-permeable hairpin polyamide pieces.

The templated reactions analyzed thus far on duplex DNA have all relied on two different reactive species. Thus, in order to pursue NCP-templated dimerizations, a single “supergroove” that has two different binding sites is needed (recall that the NCP clamp is a homodimer<sup>21</sup>). A survey of the sequences of each of the six supergrooves around the NCP crystal structure with  $\alpha$ -satellite DNA does not yield sites optimal for polyamide binding. Additionally, information about polyamide binding to each of the other supergrooves does not contain structural data of the precise positioning of polyamides. Because of these factors, it was decided to mutate two base pairs of a single

site of the supergroove to which the NCP clamp binds, thereby mutating that supergroove into a heterodimeric binding site (Figure 3.7). The site was chosen such that 6- or 8-ring

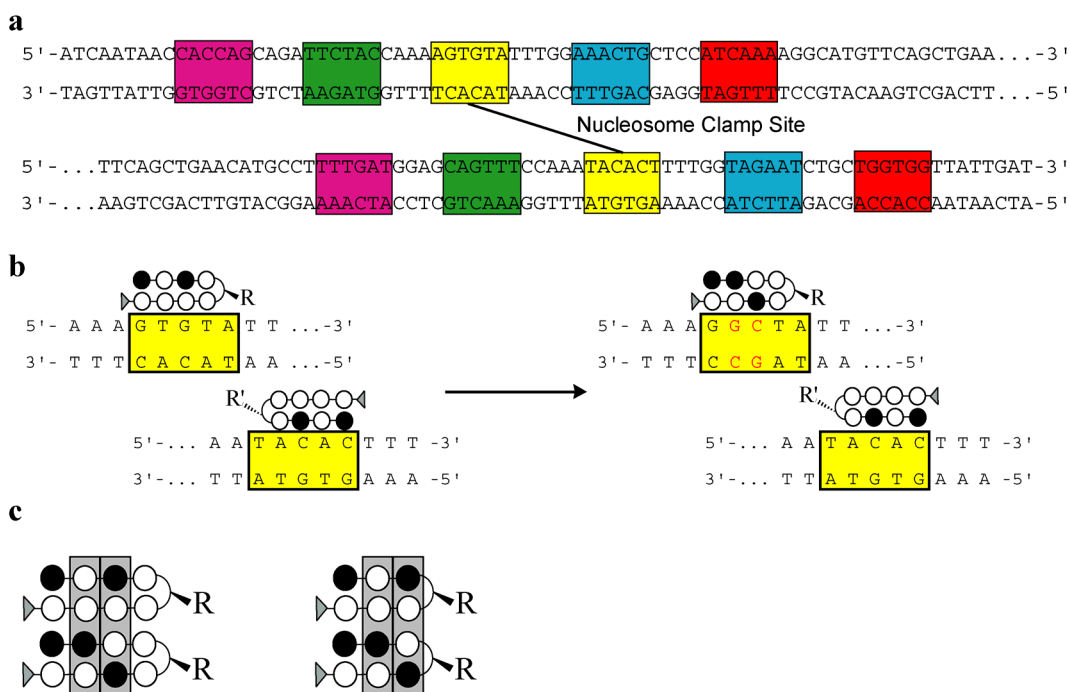
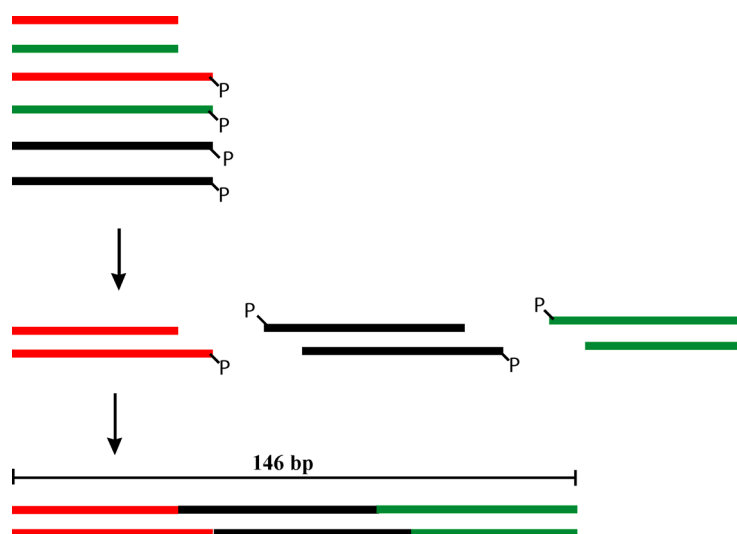


**Figure 3.7. a.** Sequence of the 146 base pair fragment of  $\alpha$ -satellite DNA used for crystallographic studies with the nucleosome clamp. In those structures, the clamp was found to bind in the homodimeric “supergroove” highlighted in yellow. Each of the other four supergrooves on the NCP are highlighted in purple, green blue and red. **b.** Highlight of the sequences to which the nucleosome clamp was bound (left). At right is shown the two base pair mutation (in red) introduced so that the supergroove becomes heterodimeric. Located above each highlighted site is the polyamide designed to target that site. **c.** Illustration of the fact that both 8-ring and 6-ring hairpin polyamides can be designed for the new supergroove sequence (**b**, right). In each case, the two polyamides differ from each other by a double base pair mismatch (highlighted in gray).

hairpin polyamides could be designed to bind the sites. In each case, the two molecules differ from each other by a double base pair mismatch. Additionally, the sites were designed such that the 6-ring polyamides that match the sites are the same polyamides used the duplex template study described above. Thus, new 6-ring polyamides will not need to be synthesized for this study. One additional concern is that because nucleosome positioning is very important to this study, it is hoped that this small perturbation does not affect the character of this DNA that causes it to be well-positioned.

We will introduce the mutated bases by a combination of chemical synthesis and biochemical techniques. The schematic for creation of the 146 base pair fragment is outlined in Scheme 3.1. Briefly, three ~50mers of duplex DNA will be chemically synthesized. Each will have an overhanging 4 base pair region that is complementary to the strand to which it is to be ligated. T4 DNA ligase will then be used to stitch the three pieces together. Once small quantities of the full 146mer have been synthesized, polymerase chain reaction (PCR) will be used to obtain sufficient quantities for kinetic assays. With the DNA in hand, NCPs will be reconstituted and incubated with functionalized hairpin polyamides, and dimer product formation monitored by quantitation of analytical HPLC traces.



**Scheme 3.1.** Schematic of the semisynthesis of the 146 base pair fragment of DNA for NCP-mediated ligation studies. Six ~50mers will be chemically synthesized, four being 5'-phosphorylated (sequences represented by red, green, and black lines; complementary sequences are the same color.). Complementary sequences will be annealed. Sequences are designed such that the resulting duplexes have four base pair overhangs that are complementary to the overhangs on the duplexes to which they will be ligated (i.e., red overhang is complementary to the left black overhang; right black overhang is complementary to the green overhang). T4 DNA ligase will then be used to stitch the entire 146 base pair fragment together. PCR will be used to amplify the fragment to obtain amounts necessary for kinetic studies.

### Profluorescent Azidocoumarins: Fluorescent Readout of Dimerizations.

Recently, researchers showed that installation of an azide into the 3- position of coumarins quenches fluorescence. Upon reaction of the azide with alkynes via a 1,3-dipolar cycloaddition, fluorescence is restored (Figure 3.8).<sup>32</sup> By functionalizing

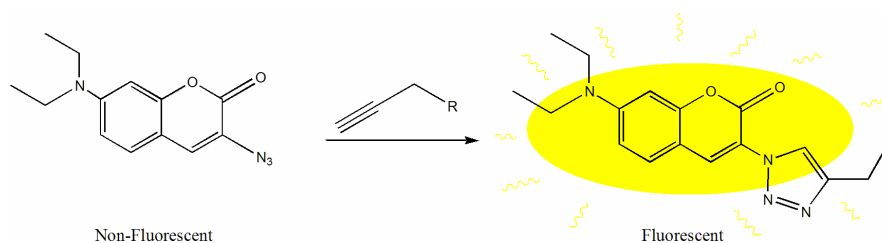


**Figure 3.8.** Representation of fluorescence rescue by 1,3-dipolar cycloadditions. 3-azidocoumarins are non-fluorescent because the lone pairs on the azide moiety are able to donate back into the ring and quench the excited state. Upon reaction with an alkyne, the electron-withdrawing triazole no longer quenches the excited state, and coumarin fluorescence is restored.

polyamides designed to the NCP “supergroove” with a 3-azidocoumarin and an alkyne, fluorescence rescue can be used as a readout for templated dimerization (Figure 3.9). Templated dimerizations can thus be monitored (even from the insides of living cells) in a non-invasive fashion via fluorescence microscopy.

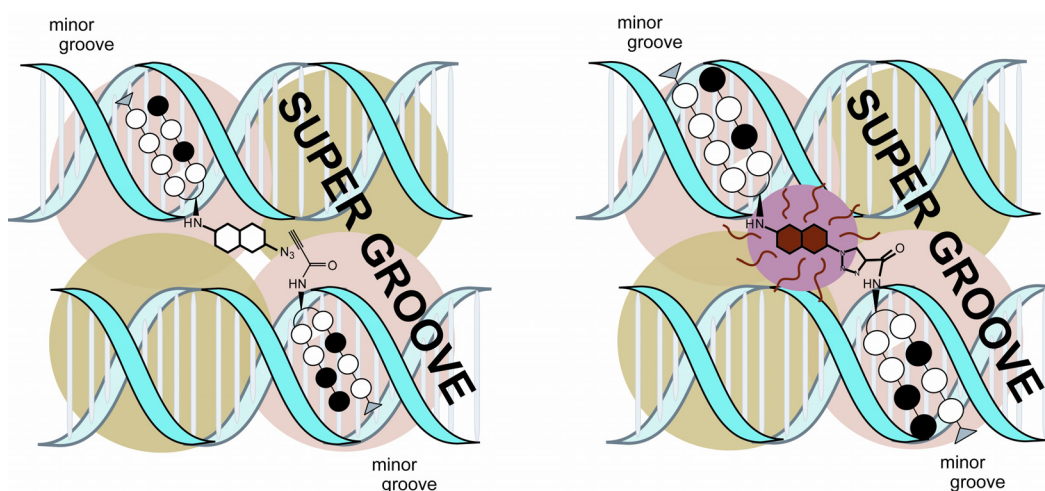


**Figure 3.9.** Schematic of fluorescence rescue by NCP-mediated polyamide dimerization. Azidocoumarin- and alkyne-functionalized polyamides bind to a “supergroove” (right), placing the reactive groups in close proximity. The templated cycloaddition then forms the fluorescent polyamide dimer product (left).

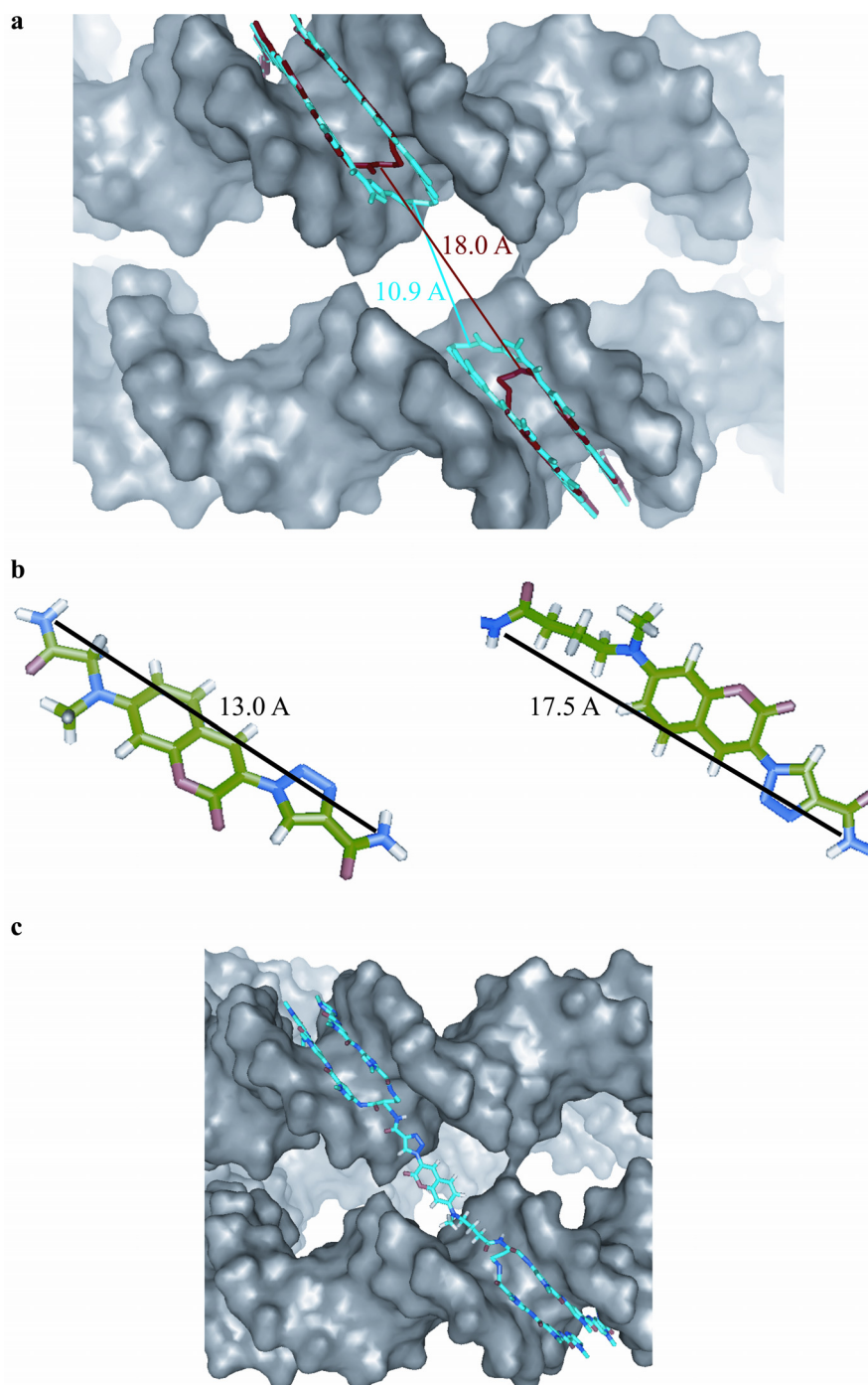


**Figure 3.10.** a. X ray crystal structure of 8-ring (blue) polyamides bound to the “supergroove” highlighting the 11 Å distance between hairpins. When 6-ring polyamides are modeled in (red), the distance between polyamides is increased to 18 Å. b. Energy-minimized models of triazole-coumarin linkers with 1 (left) and 3 (right) methylene spacers. Labeled atomic distances show these linkers to be good fits for the gap between hairpins bound to the NCP supergroove. Green = carbon, white = hydrogen, blue = nitrogen, red = oxygen. c. Model of the longer triazole coumarin linker forming a dimer between two 6-ring hairpin polyamides bound to a single supergroove.

In order to establish the feasibility of this scheme, molecular modeling was done to verify that the coumarin-triazole linker would appropriately span the gap across the two gyres of DNA on the NCP. A model of the triazole-coumarin linker was built in the Spartan ES software package and energy-minimized using an AM1 model, followed by *ab initio* calculations by means of the Hartree-Fock model and a 6-31G\* basis set. As shown in Figure 3.10, the fully extended structure of the shortest triazole-coumarin spans 13 Å. This distance approximates the 10.99 Å distance between the two polyamide turn amines in the crystal structure. When 6-ring hairpin polyamides are substituted for the 8-ring polyamides on the crystal structure, the distance between turn amines increases to 17.8 Å. A triazole-coumarin linker formed from an alkynyl amide and an azidocoumarin functionalized with a three-carbon linker creates an approximately 18 Å linker. Thus, modeling shows that triazole-coumarins can be accommodated by the gap between hairpin binding sites within a single NCP supergroove.

### **Towards synthesis of functionalized 3-azidocoumarins.**

Based on our previous templating work, it is clear that the kinetics of templated 1,3-dipolar cycloadditions are most favorable when alkynes directly conjugated to an electron-withdrawing group are used. While previous literature shows alkyl alkynes capable of fluorescence rescue, it does not offer any information on whether alkynyl amidates can be used with 3-azidocoumarins to rescue fluorescence. As initial controls, in separate reactions, 7-diethylamino 3-azidocoumarin was combined with **5** and **7**, and allowed to react at room temperature under copper-mediated conditions.<sup>33</sup> After two hours, reactions were deemed complete by HPLC. Solutions of the starting material and

products were irradiated with 365 nm light. As shown qualitatively in Figure 3.11, the products are intensely fluorescent with respect to the 3-azidocoumarin starting material. Thus, alkynyl amidates can be used to rescue the fluorescence of 3-azidocoumarins via a 1,3-dipolar cycloaddition.

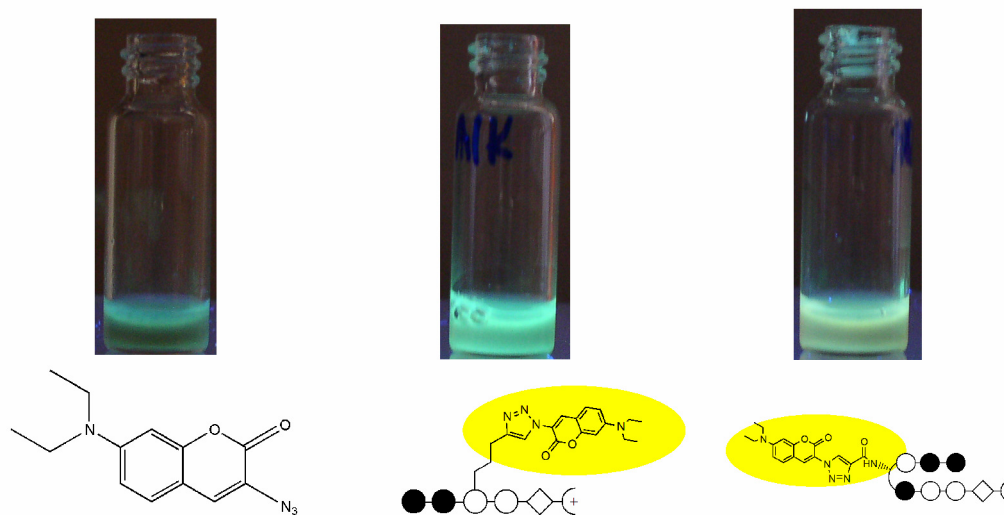


**Figure 3.11.** Aqueous solutions of azidocoumarin (left), alkyl triazole coumarin (center), and alkynyl amidate triazole coumarin (right) illuminated with 365 nm light. As shown, the azidocoumarin is relatively non-fluorescent, while the two triazole coumarins are intensely fluorescent.

With the necessary controls performed, our attention was turned towards synthesis of a 3-azidocoumarin that could be conjugated to a polyamide. Figure 3.12 shows our planned synthetic scheme and our progress towards this molecule. The decision was made to create azidocoumarins with a tertiary amine in the 7 position, since these molecules have been shown to be the most intensely fluorescent.<sup>32</sup> To begin the synthesis, *m*-aminophenol is mono-*N*-methylated by stepwise formylation and reduction to yield compound **17**.<sup>34</sup> The secondary amine is then alkylated with methylbromoacetate to yield tertiary amine **18** with a protected handle for linkage to a polyamide.<sup>35</sup> Formylation of the aromatic ring is accomplished under Vilsmier conditions to yield

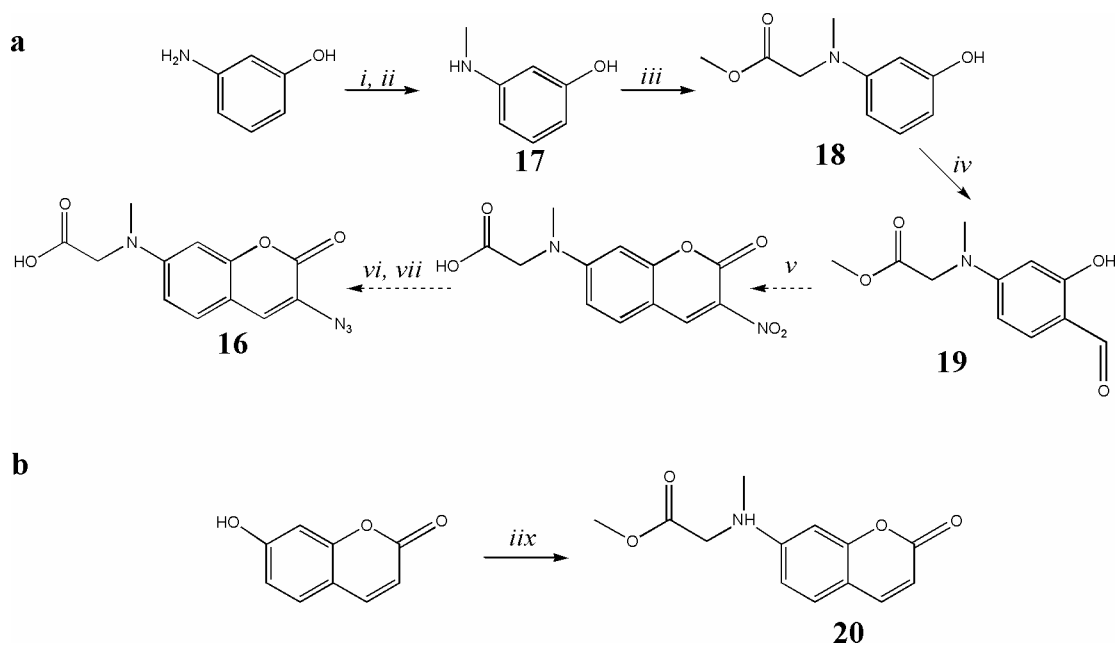


**Figure 3.12.** **a.** Synthetic scheme for an azidocoumarin that can be attached to a polyamide. i) ethyl formate, reflux, ii)  $\text{BH}_3$ -THF, THF (60% for two steps), iii) methyl bromoacetate, 2,6 lutidine, DMF (85%), iv)  $\text{POCl}_3$ , DMF (35%), v) nitro ethyl acetate, pyridine, acetic acid, toluene, vi)  $\text{SnCl}_2$ , HCl, vii)  $\text{NaNO}_2$ , KOAc,  $\text{NaN}_3$ . **b.** Buchwald coupling to install secondary amine functionality, iix) N-phenyl triflimide; then,  $\text{Pd}_2(\text{dba})_3$ , *rac*-BINAP,  $\text{Cs}_2\text{CO}_3$ , sarcosine methyl ester, toluene (12% for two steps). Dashed arrows indicate reactions yet to be run.

compound **19**.<sup>35</sup> Following standard procedures,<sup>32</sup> the nitro coumarin should be readily accessible, which can then be converted into the functionalized azidocoumarin **16**.

In our studies towards these functionalized 3-azidocoumarins, we initially pursued installation of the tertiary amine, in one step, from triflated 7-hydroxycoumarin via a palladium-mediated Buchwald coupling.<sup>36</sup> Transformations on the model system were performed with N-methyl sarcosine. While product was detected, yields were quite low, and the decision was made to follow the above route. It should be noted that Buchwald reactions were not optimized for this study, and future attention may be paid to synthetic routes utilizing this reaction.

Thus, significant progress has been made towards NCP-mediated dimerizations of hairpin polyamides, as well as towards a system in which dimerization can be monitored by fluorescence. It should be noted that for NCP-mediated dimerizations involving 6-

ring hairpin polyamides, compounds **1–15** are complementary to the designed supergroove sites and can be used without further synthesis.

## Discussion

Initial experiments were designed to determine whether duplex DNA could template the dimerizations of hairpin polyamides in a turn-to-turn orientation. A panel of thermal, water-tolerant reactions was screened against duplex DNA templates with binding sites ranging from 10 to 13 base pairs. In order for templated reactions to be useful in *in vivo* experiments, reactive partners must not react in solution, but must form significant product in a biologically relevant time scale. On duplex DNA, only the Huisgen 1,3-dipolar cycloaddition between an ethyl azide and a terminal alkynyl amidate (**3 + 5**) fits the above criteria.

The cycloaddition between **3** and **5** shows excellent efficiency on the 10 base pair template, achieving almost 50% yield in eight hours, and eventually reaching 78% completion in 24 hours. This represents an almost 25,000-fold increase in rate from the nontemplated reaction. While the turn-to-turn templated reaction is more efficient than its turn-to-tail counterpart,<sup>20</sup> it exhibits reduced site-separation specificity, reacting to modest yields on the 11 base pair site as well.

It was hypothesized that for the templated turn-to-tail dimer forming reactions<sup>20</sup> at 1  $\mu\text{M}$ , product formation on the mismatch template was due to the ability of the polyamides to bind their mismatch sites at these high concentrations. When the concentration is decreased, the polyamides are better able to selectively bind the match site, and product formation on the mismatch templates is reduced. While the site

separation specificity is not great for the turn-to-turn dimerization reaction, the template mismatch specificity is exquisite. At 500 nM concentrations, the reaction proceeds on the match template more than an order of magnitude (11-fold) more efficiently than on the mismatch template.

With respect to the 1,3-dipolar cycloaddition between **3** and the methyl alkyne **6**, it is interesting that no reaction is observed on the 11 base pair template, even though the reactive species are identical in length to **3** and **5**. Perhaps on the longer 11 base pair template, the reactive groups are fully stretched out, and the transition state pushes the terminal methyl group into one of the walls or the floor of the minor groove, whereas at the shorter 10 base pair template, the linker is able to fold slightly to avoid such a steric clash.

The 1,3-dipolar cycloadditions between the bulky phenyl azide and the various alkynes did not proceed on duplex templates. Previous researchers have found that phenyl azides are more reactive than alkyl azides in these cycloadditions.<sup>37, 38</sup> Thus, the lack of reactivity must be due to some steric constraint imposed upon the reaction by sequestration in the minor groove. This reaction offers great potential for a supergroove-specific, turn-to-turn, dimer-forming reaction.

With respect to the other reactions tried, several interesting features emerge. First, the Wittig reaction does not proceed on any of the templates. The Wittig starting materials each contain bulky phenyl rings, with polyamide **15** containing the extremely bulky triphenylphosphine moiety. It is not surprising then, that this pairing produces no reaction within the narrow confines of the minor groove of the duplex templates. Perhaps

when the reaction is tried across the more sterically free nucleosomal supergroove, product will be observed.

Similarly, the Diels-Alder reactions result in bulky fused ring systems that may be incompatible within the narrow confines of the minor groove. That no templated reaction was observed may be due to a sterically large transition state that can not fit within the minor groove. Because the Diels-Alder reactions produce no product under non-templated conditions, these may be ideal reactions for dimer formation on nucleosomal supergroove templates that will not impose as stringent steric constraints on the transition state as duplex template.

With respect to the Michael additions, it is unfortunate that the reaction proceeds at 1  $\mu\text{M}$  concentrations in the absence of template. Because of the significant non-templated product formation, this reaction cannot be used for dimerization across “supergroove” templates. It does appear that templates **A** and **B** were able to increase the yield (and by extension, rate) of product formation, however, the non-templated background rate is too high to warrant its use for biological applications. It is interesting that on the longer templates, these reactions do not produce any product. Perhaps the polyamides are bound to the minor groove, effectively sequestering the reactive groups in a geometry that does not allow the reactive species to interact, thereby inhibiting product formation.

### **Conclusion.**

Linear, duplex DNA is able to template the formation of turn-to-turn hairpin dimers. While a panel of reactions was examined, only the 1,3-dipolar cycloaddition

between an alkyl azide and an alkynyl amidate proceeded in good yields and with good site-size and mismatch selectivity. At micromolar concentrations, duplex template enhances the rate of a dipolar cycloaddition between **3** and **5** 20,000-fold. Because turn-functionalized polyamides have been shown to have increased nuclear uptake ability relative to their tail-functionalized counterparts, this scaffold offers the opportunity to be used for the *in vivo* creation of hairpin dimers, potentially using the promoter of interest to guide formation of a molecule able to influence cell function.

## Materials and Methods.

### 3-azido propionic acid (**3a**)<sup>39</sup>

Sodium azide (897 mg, 13.8 mmol) was dissolved in 5 mL water at 10 °C. Keeping the temperature under 25 °C,  $\beta$ -propiolactone (1 g, 13.8 mmol) was added portion-wise. The reaction was stirred at rt for 4 h, after which 8 mL of 37% HCl was added. The product was extracted with diethyl ether (3 x 20 mL). The combined extracts were dried over Na<sub>2</sub>SO<sub>4</sub>, and concentrated by rotary evaporation under reduced pressure. Spectra as reported in Leffeler, et al.<sup>39</sup>

### Polyamide **3**

Polyamide **1** (2  $\mu$ mol) was combined with **3a** (3  $\mu$ mol), PyBOP (3  $\mu$ mol), and DIEA (20  $\mu$ mol) in 300  $\mu$ L anhydrous DMF at rt for 1 h. Reaction was quenched by addition of 9 mL 0.1% TFA in water, and purified by reversed phase HPLC for a final yield of 45%. UV (H<sub>2</sub>O)  $\lambda_{\text{max}}$  310 nm (51540). MALDI-TOF-MS calcd. (M + H): 1020.1. Found 1019.6.

**Polyamide 4**

Synthesized from polyamide **1** (1  $\mu\text{mol}$ ) and the p-azido benzoic acid NHS-ester (Pierce, 2  $\mu\text{mol}$ ) in 200  $\mu\text{L}$  10:1 DMF:DIEA. Reaction was quenched by addition of 9 mL 0.1% TFA in water, and purified by reversed phase HPLC for a final yield of 72%. UV ( $\text{H}_2\text{O}$ )  $\lambda_{\text{max}}$  310 nm (51540). MALDI-TOF-MS calcd. (M + H): 1067.5. Found 1067.8.

**Polyamide 5**

For preparation, see Chapter 2 of this thesis.

**Polyamide 6**

Synthesized as **3** from 2-butynoic acid for an overall yield of 35%. UV ( $\text{H}_2\text{O}$ )  $\lambda_{\text{max}}$  310 nm (51540). MALDI-TOF-MS calcd. (M + H): 1060.5. Found 1060.8.

**Polyamide 7**

For preparation, see Chapter 2 of this thesis.

**Polyamide 8**

Synthesized as **4** from the NHS ester of  $\gamma$ -maleimido butyric acid (Pierce) for a 70% overall yield. UV ( $\text{H}_2\text{O}$ )  $\lambda_{\text{max}}$  310 nm (51540). MALDI-TOF-MS calcd. (M + H): 1088.3. Found 1088.3.

**Polyamide 9**

Synthesized as **3** from 2-furyl propionic acid for a 64% overall yield. UV (H<sub>2</sub>O)  $\lambda_{\max}$  310 nm (51540). MALDI-TOF-MS calcd. (M + H): 1141.5. Found 1141.8.

**Polyamide 10**

Synthesized as **3** from Boc- $\beta$ -alanine, followed by deprotection with 50% TFA:DCM for a 41% overall yield. UV (H<sub>2</sub>O)  $\lambda_{\max}$  310 nm (51540). MALDI-TOF-MS calcd. (M + H): 1066.1. Found 1066.6.

**Polyamide 11**

Synthesized as **4** from the NHS ester of 1-S-acetyl acetic acid (Pierce), followed by deprotection with 2 M NaOH in 21% overall yield. UV (H<sub>2</sub>O)  $\lambda_{\max}$  310 nm (51540). MALDI-TOF-MS calcd. (M + H): 1068.5. Found 1068.5.

**Polyamide 12**

Synthesized as **4** from 4-maleimido cyclohexyl-1-carboxylic acid (Acros Organics) for a 71% overall yield. UV (H<sub>2</sub>O)  $\lambda_{\max}$  310 nm (51540). MALDI-TOF-MS calcd. (M + H): 1044.5. Found 1044.7.

**Polyamide 13**

Synthesized as **12** for a 71% overall yield. UV (H<sub>2</sub>O)  $\lambda_{\max}$  310 nm (51540). MALDI-TOF-MS calcd. (M + H): 1116.5. Found 1116.5.

**Polyamide 14**

Synthesized as **4** from Salicaldehyde (Aldrich) for a 54% overall yield. UV (H<sub>2</sub>O)  $\lambda_{\text{max}}$  310 nm (51540). MALDI-TOF-MS calcd. (M + H): 1054.5. Found 1054.7.

**Polyamide 15**

Polyamide **2** was combined with the NHS ester of 4-iodoaminoacetic acid (SIAB, Pierce), according to **4**. After HPLC purification and lyophilization, product was mixed with 4-(diphenylphosphino) benzoic acid in 3:7 MeOH:THF for 8 h at 55 °C for a two step yield of 12% . UV (H<sub>2</sub>O)  $\lambda_{\text{max}}$  310 nm (51540). MALDI-TOF-MS calcd. (M + H): 1459.2. Found 1459.6.

**17**

2-aminophenol (5 g, 47.6 mmol) was refluxed in ethyl formate (75 mL) for 48 h. The reaction was concentrated by rotary evaporation, and the product purified by silica gel chromatography (1:1 EtOAc:Hexanes) (3 g, 25 mmol, 51 % yield). The resulting purified product (540 mg, 3.96 mmol) was dissolved in 30 mL dry THF and cooled to 0 °C. 11.3 mL of a 1 M solution of BH<sub>3</sub>-THF was added via syringe. The reaction was stirred at 0 °C for 1 h and then rt for 1.5 h. The reaction was quenched by the addition of 8 mL 10% citric acid. The product was extracted with EtOAc (5 x 20 mL). The combined organic layer was washed with brine (2 x 30 mL), dried over anhydrous Na<sub>2</sub>SO<sub>4</sub>, and concentrated by rotary evaporation. Product was purified by silica gel

chromatography (430 mg, 86% yield).  $^1\text{H}$  NMR in  $\text{CDCl}_3$   $\delta$  7.0 m 1H, 6.2 m 2H, 6.08 m 1H, 2.79 s 3H, 2.05 s 1H.

## 18

Compound **17** (100 mg, 0.812 mmol) was dissolved in DMF (3 mL). 2,6 lutidene (600  $\mu\text{L}$ ) and methylbromoacetate (150  $\mu\text{L}$ , 0.934 mmol) were added and the reaction stirred at rt for 20 h. The reaction was concentrated by rotary evaporation and the product purified by silica gel chromatography (2:1 Hexanes:EtOAc). Product was isolated as a white powder (163 mg, 0.69 mmol, 85%).  $^1\text{H}$  NMR in  $\text{CDCl}_3$   $\delta$  7.0 t 1H, 6.15 m 3H, 6.0 s, 1H, 3.82 s 2H, 3.21 s 3H, 1.56 s 3H.

## 19

Compound **18** (160 mg, 0.675 mmol) was dissolved in 1 mL DMF.  $\text{POCl}_3$  (103 mg, 0.675 mmol) and DMF (492 mg, 6.75 mmol) were combined in a separate flask and stirred under  $\text{N}_2$  at 0  $^\circ\text{C}$  for 1 h and then rt for 1.5 h. This mix was then cannulated into the stirring solution of **18**. The reaction was then stirred at rt for 48 h. The reaction was quenched with 10 mL of 0.5 M NaOH. The pH was then adjusted to 7.0 and the product extracted into EtOAc. The combined organic layer was washed with brine, dried over sodium sulfate and concentrated by rotary evaporation. The product was isolated as a clear oil after silica gel chromatography (2:1 Hexanes:EtOAc, 60 mg, 35%).  $^1\text{H}$  NMR in  $\text{CDCl}_3$   $\delta$  11.3 s 1H, 9.28 s 1H, 7.14 d 1H, 6.0 d 1H, 5.9 dd 1H, 3.95 s 2H, 3.31 s 3H, 1.62 s 3H.

**Template-Derived Masses for Dimer Products.**

**3 + 5** - MALDI-TOF-MS calcd. (M + H): 2067.7. Found 2067.6.

**3 + 6** - MALDI-TOF-MS calcd. (M + H): 2080.9. Found 2081.4.

**3 + 7** - MALDI-TOF-MS calcd. (M + H): 2093.9. Found 2093.6.

**8 + 10** - MALDI-TOF-MS calcd. (M + H): 2155.2. Found 2156.0.

**8 + 11** - MALDI-TOF-MS calcd. (M + H): 2152.4. Found 2178.2 [M+H+19]<sup>+</sup>

(corresponds to hydrolyzed maleimide).

**Sample Buchwald Coupling Procedures (20)**

7-hydroxycoumarin (500 mg, 3.08 mmol) was combined in THF (20 mL) with triethylamine (429  $\mu$ L, 3.08 mmol) and stirred for 5 min. N-phenyltriflimide (1.1 g, 3.08 mmol) was then added and the reaction stirred under inert atmosphere for 3 h at rt. The reaction was concentrated and the residue purified by silica gel chromatography (3:1 Hexanes:EtOAc). Product was isolated as a white powder (760 mg, 83%). In a flame-dried flask, the triflated material (100 mg, 0.34 mmol), Cs<sub>2</sub>CO<sub>3</sub> (220 mg, 0.68 mmol), ( $\pm$ )-BINAP (32 mg, 0.051 mmol), Pd<sub>2</sub>(dba)<sub>3</sub> (35 mg, 0.034 mmol), and N-methyl glycine methyl ester (57 mg, 0.41 mmol) were combined and dried under vacuum for 2 h. Toluene (3 mL) was then added, and the mixture stirred at 80 °C for 14 h. The reaction mixture was filtered, and the ppt. washed with DCM. The combined filtrates were concentrated by rotary evaporation, and the product chromatographed in 1.5:1 Hexanes:EtOAc. The product (**20**) was isolated as a bright yellow oil (10 mg, 12% yield).

**Preparation of duplex DNA for kinetic experiments.** Duplex DNA was prepared by incubating equal amounts of complementary sets of synthetic oligonucleotides at 90 °C for 10 min, then slowly allowing them to cool to rt. Resulting duplex DNA was quantified by UV by the relationship 1 OD<sub>260</sub> unit = 50 µg/mL duplex DNA. Duplex DNA was stored at -20 °C in water.

**Typical Reaction Procedure.** All kinetic reactions were performed in 1.7 mL presiliconized microcentrifuge tubes obtained from VWR International. Total reaction volumes were 1.2 mL aqueous solutions of equimolar concentrations of each hairpin polyamide and DNA (2 mM Tris-HCl, 2 mM KCl, 2 mM MgCl<sub>2</sub>, 1 mM CaCl<sub>2</sub>, pH 7.0, 37 °C). Reactions were monitored by HPLC by direct injection of reaction samples onto a RAINEN C<sub>18</sub>, Microsorb MV, 5 µm, 300 x 4.6 mm reversed-phase column in 0.1% (w/v) TFA-H<sub>2</sub>O with acetonitrile as eluent and a flow rate of 1.0 mL/min, gradient elution 0.5% CH<sub>3</sub>CN/min. Peaks were quantified using the Beckman Coulter GOLD software package. Verification of product was determined by MALDI TOF-MS of ~40 µL samples of each reaction concentrated on a ZipTip 2 mg C<sub>18</sub> pipette tip eluted with 75% (v/v) acetonitrile in 0.1% (w/v) TFA.

**References.**

1. Dervan, P. B., *Science*, **1986**, 232, 464–471.
2. Dervan, P. B., *Bioorganic & Medicinal Chemistry*, **2001**, 9, 2215–2235.
3. Dervan, P. B.; Edelson, B. S., *Current Opinion in Structural Biology*, **2003**, 13, 284–299.
4. Olenyuk, B. Z.; Zhang, G. J.; Klco, J. M.; Nickols, N. G.; Kaelin, W. G.; Dervan, P. B., *Proceedings of the National Academy of Sciences of the United States of America*, **2004**, 101, 16768–16773.
5. Livengood, J. A.; Fechter, E. J.; Dervan, P. B.; Nyborg, J. K., *Frontiers in Bioscience*, **2004**, 9, 3058–3067.
6. Nguyen-Hackley, D. H.; Ramm, E.; Taylor, C. M.; Joung, J. K.; Dervan, P. B.; Pabo, C. O., *Biochemistry*, **2004**, 43, 3880–3890.
7. Fechter, E. J.; Dervan, P. B., *Journal of the American Chemical Society*, **2003**, 125, 8476–8485.
8. Ehley, J. A.; Melander, C.; Herman, D.; Baird, E. E.; Ferguson, H. A.; Goodrich, J. A.; Dervan, P. B.; Gottesfeld, J. M., *Molecular and Cellular Biology*, **2002**, 22, 1723–1733.
9. Bremer, R. E.; Wurtz, N. R.; Szewczyk, J. W.; Dervan, P. B., *Bioorganic & Medicinal Chemistry*, **2001**, 9, 2093–2103.
10. Chiang, S. Y.; Burli, R. W.; Benz, C. C.; Gawron, L.; Scott, G. K.; Dervan, P. B.; Beerman, T. A., *Journal of Biological Chemistry*, **2000**, 275, 24246–24254.
11. Dickinson, L. A.; Trauger, J. W.; Baird, E. E.; Dervan, P. B.; Graves, B. J.; Gottesfeld, J. M., *Journal of Biological Chemistry*, **1999**, 274, 12765–12773.
12. Best, T. P.; Edelson, B. S.; Nickols, N. G.; Dervan, P. B., *Proceedings of The National Academy of Sciences of the United States of America*, **2003**, 100, 12063–12068.
13. Edelson, B. S.; Best, T. P.; Olenyuk, B.; Nickols, N. G.; Doss, R. M.; Foister, S.; Heckel, A.; Dervan, P. B., *Nucleic Acids Research*, **2004**, 32, 2802–2818.
14. Bailly, C.; Chaires, J. B., *Bioconjugate Chemistry*, **1998**, 9, 513–538.
15. Faria, M.; Giovannangeli, C., *Journal of Gene Medicine*, **2001**, 3, 299–310.
16. Reddy, B. S. P.; Sharma, S. K.; Lown, J. W., *Current Medicinal Chemistry*, **2001**, 8, 475–508.

17. Herman, D. M.; Baird, E. E.; Dervan, P. B., *Chemistry-a European Journal*, **1999**, *5*, 975–983.
18. Kers, I.; Dervan, P. B., *Bioorganic & Medicinal Chemistry*, **2002**, *10*, 3339–3349.
19. Weyermann, P.; Dervan, P. B., *Journal of the American Chemical Society*, **2002**, *124*, 6872–6878.
20. Poulin-Kerstien, A. T.; Dervan, P. B., *Journal of the American Chemical Society*, **2003**, *125*, 15811–15821.
21. Edayathumangalam, R. S.; Weyermann, P.; Gottesfeld, J. M.; Dervan, P. B.; Luger, K., *Proceedings of the National Academy of Sciences of the United States of America*, **2004**, *101*, 6864–6869.
22. Poulin-Kerstien, A. T. DNA-Templated Dimerizations of Minor Groove-Binding Polyamides. California Institute of Technology, Pasadena, 2005.
23. Calderone, C. T.; Puckett, J. W.; Gartner, Z. J.; Liu, D. R., *Angewandte Chemie-International Edition*, **2002**, *41*, 4104–4108.
24. Gartner, Z. J.; Kanan, M. W.; Liu, D. R., *Angewandte Chemie-International Edition*, **2002**, *41*, 1796–1798.
25. deClairac, R. P. L.; Geierstanger, B. H.; Mrksich, M.; Dervan, P. B.; Wemmer, D. E., *Journal of the American Chemical Society*, **1997**, *119*, 7909–7916.
26. Kielkopf, C. L.; Baird, E. E.; Dervan, P. D.; Rees, D. C., *Nature Structural Biology*, **1998**, *5*, 104–109.
27. Kielkopf, C. L.; White, S.; Szewczyk, J. W.; Turner, J. M.; Baird, E. E.; Dervan, P. B.; Rees, D. C., *Science*, **1998**, *282*, 111–115.
28. Suto, R. K.; Edayathumangalam, R. S.; White, C. L.; Melander, C.; Gottesfeld, J. M.; Dervan, P. B.; Luger, K., *Journal of Molecular Biology*, **2003**, *326*, 371–380.
29. Baird, E. E.; Dervan, P. B., *Journal of the American Chemical Society*, **1996**, *118*, 6141–6146.
30. Belitsky, J. M.; Nguyen, D. H.; Wurtz, N. R.; Dervan, P. B., *Bioorganic & Medicinal Chemistry*, **2002**, *10*, 2767–2774.
31. Davey, C. A.; Sargent, D. F.; Luger, K.; Maeder, A. W.; Richmond, T. J., *Journal of Molecular Biology*, **2002**, *319*, 1097–1113.
32. Sivakumar, K.; Xie, F.; Cash, B. M.; Long, S.; Barnhill, H. N.; Wang, Q., *Organic Letters*, **2004**, *6*, 4603–4606.

33. Rostovtsev, V. V.; Green, L. G.; Fokin, V. V.; Sharpless, K. B., *Angewandte Chemie-International Edition*, **2002**, *41*, 2596–2599.
34. Nakagawa, Y.; Irie, K.; Masuda, A.; Ohigashi, H., *Tetrahedron*, **2002**, *58*, 2101–2115.
35. Feuster, E. K.; Glass, T. E., *Journal of the American Chemical Society*, **2003**, *125*, 16174–16175.
36. Muci, A. R.; Buchwald, S. L., Practical palladium catalysts for C-N and C-O bond formation. In *Cross-Coupling Reactions*, 2002; Vol. 219, pp 131–209.
37. Huisgen, R., *1,3-Dipolar Cycloaddition Chemistry*. Wiley-Interscience: New York, 1984; p Chapter 1.
38. Huisgen, R., *Profiles, Pathways, and Dreams*. American Chemical Society: Washington, DC, 1994.
39. Leffler, J. E.; Temple, R. D., *Journal of the American Chemical Society*, **1967**, *89*, 5235–5246.